

## Polyfullerene Thin Films Applied as NH<sub>3</sub> Sensors

André Vítor Santos Simões<sup>a\*</sup> , Lucas Kaique Martins Roncaselli<sup>a</sup>,

Vinícius Jessé Rodrigues de Oliveira<sup>a</sup> , Maria Eduarda Rocha Santos Medina<sup>a</sup>,

Hasina H. Ramanitra<sup>b</sup>, M. Stephen<sup>b</sup>, Deuber L. Silva Agostini<sup>a</sup>, Roger C. Hiorns<sup>b</sup>,

Clarissa de Almeida Olivati<sup>a</sup>

<sup>a</sup>Universidade Estadual Paulista, Presidente Prudente, SP, Brasil.

<sup>b</sup>University of Pau and Pays de l'Adour, Institute of Analytical Sciences and Physico-Chemistry for Environment and Materials, 64000, Pau, France.

Received: August 29, 2021; Accepted: September 23, 2021

Fullerene is considered to be the third carbon allotrope after diamond and graphite. The study of fullerene derivatives has been growing due to their exceptional electron affinity. This work proposes the study of three different fullerene derivatives, being phenyl-C<sub>61</sub>-butyric acid methyl ester (PCBM), oligo {(phenyl-C<sub>61</sub>-butyric acid methyl ester)-alt-[1,4-bis(bromomethyl)-2,5-bis(octyloxy)benzene]} (OPCBMMB) and poly {[bispyrrolidino(phenyl-C<sub>61</sub>-butyric acid methyl ester)]-alt-[2,5-bis(octyloxy)benzene]} (PPCBMB), and their application as NH<sub>3</sub> sensors. Experimental results showed that these materials have a reproducible response to NH<sub>3</sub>, with PCBM resulting in the highest observed current peak, followed by OPCBMMB and PPCBMB. These results imply that PCBM, OPCBMMB and PPCBMB can be used to produce NH<sub>3</sub> sensors.

**Keywords:** Fullerene, NH<sub>3</sub>, Gas sensors.

### 1. Introduction

The ease and low cost of processing has made polymeric materials abundantly present in our daily lives. In the electrical industry, polymeric materials were initially used in order to replace paper-based insulators. Their acceptance was rapid because they are light, cheap and highly insulating materials<sup>1</sup>.

The discovery of buckminsterfullerene (C<sub>60</sub>) in 1985, more commonly known as fullerene, occurred accidentally in an attempt to simulate the conditions of nucleation of carbon atoms in cold red giant N-type stars<sup>2</sup>. Because of its structural stability, C<sub>60</sub> is considered to be the third carbon allotrope, after diamond and graphite<sup>3</sup>.

One of the problems associated with fullerene is its very strong tendency to aggregate in an uncontrolled manner. This means that its sensor, electronic and medical properties can be hard to exploit. A route around this problem can be provided by incorporating fullerene into a polymeric structure. This means that its aggregation becomes more controlled, its solubility in common solvents is improved, and as a material it becomes more malleable and easier to handle. One of the simplest ways of incorporating fullerene into a polymer is to use it like a monomer and make it part of the polymer 's back-bone. This can be done via several routes, notably by copolymerization with comonomers via radical<sup>4</sup> or cycloaddition<sup>5</sup> routes. These procedures can result in the production of high yields of oligo(fullerene)s and poly(fullerene)s that contain high proportions of fullerene (typically > 60% by weight).

Gas sensors are mostly composed by p-type materials, such as P3HT, however, n-type materials have been relatively ignored and are not so well understood<sup>6</sup>. Fullerenes are of particular interest due to their structural stability and their exceptional affinity for electrons<sup>7,8</sup>.

The study of the interaction between gas molecules and semiconductors is one of the most studied areas and has attracted the attention of many researchers. Monitoring gases play a high importance role, especially toxic gases of our daily life. Gas sensors are also commonly used as safety devices, especially in industrial areas where toxic chemical compounds might leak. One example is NH<sub>3</sub> which is an important part of the atmosphere and plays the role of neutralizing acid gases and maintaining the ecological balance<sup>9</sup>. However, NH<sub>3</sub> is also a toxic gas when at higher concentrations, especially in industrial processes and biological metabolisms<sup>10</sup>.

In this work, different poly(fullerenes) and oligo (fullerenes) were studied as thin films, made using the drop-casting deposition technique. This method was chosen as it is simple, fast and of low-cost<sup>11</sup>. It consists of simply dripping a solution of the material under study on to the substrate surface, and then evaporation the solvent. The film remains on the substrate due to Van der Waals force<sup>12,13</sup>. The drop casting technique, however, does not allow control over the formation of the film, causing the formation of uncontrolled agglomerates, resulting in films with a heterogeneous surface. Lack of control over film formation also limits control over film thickness. Some factors such as deposited volume

\*e-mail: andresimois@gmail.com

and solution concentration can help regulate the final film thickness, but with low accuracy<sup>11,14</sup>.

## 2. Methodology

### 2.1. Materials

In this work, three n-type materials were studied, being, phenyl- $C_{61}$ -butyric acid methyl ester (PCBM), oligo {(phenyl- $C_{61}$ -butyric acid methyl ester)-alt-[1,4-bis(bromomethyl)-2,5-bis(octyloxy)benzene]} (OPCBMMB) and poly {[bispyrrolidino(phenyl- $C_{61}$ -butyric acid methyl ester)]-alt-[2,5-bis(octyloxy)benzene]} (PPCBMB). Figure 1 represents the chemical structure of the studied materials. PCBM was obtained from Sigma Aldrich, OPCBMMB was prepared as detailed by Ramanitra et al.<sup>15</sup>, and PPCBMB was prepared as indicated by Stephen et al.<sup>16</sup>.

To make the thin films by drop casting deposition, solutions were made from these materials, using chloroform as the solvent at a concentration of 1.0 mg mL<sup>-1</sup>.

### 2.2. Drop casting films

Thin films based on the Drop casting technique were prepared using the polymers under study with a concentration of 0.2 mg mL<sup>-1</sup>, having chloroform as solvent. Using an electronic pipette, the solution of each material already homogenized was spread over the solid substrate on a table surface, and after 40 minutes of evaporation of the volatile solvent in a controlled environment of 22°C, a layer of the polymer could be obtained in the form of film. The solvent evaporation process is an essential part of the deposition technique, where we have the option to choose between letting

the solvent evaporate naturally or use thermal processes to accelerate the process. However, by disturbing the system, we create changes in the final morphology of the film, as stated by Kumar et al.<sup>14</sup>. In this work, we opted to let the solvent evaporate naturally. Figure 2 shows a representation of this process.

### 2.3. DC electrical characterization

The measurements of electrical characterizations in direct current (DC) and current by time ( $I$  vs  $t$ ) were performed using a Keithley 238 voltage source.

After deposition of the films on Interdigitated gold electrodes (IDE-Au) that has the characteristics of:  $N = 50$  digits with dimensions of 110 mm high ( $h$ ), 8 mm long ( $L$ ) and 100  $\mu\text{m}$  wide ( $w$ ), as shown in Figure 3.

The films were subjected to current by voltage measurements ( $I$  vs  $V$ ), varying the applied potential from -15 to 15 Volts, before and after measurements with  $\text{NH}_3$  vapor, to verify the electrical conductivity of the material and the electrochemical effect of the interaction.

The measurements of current over time with the same samples are the stage in which the films were exposed to the steam flow, which in contact with the films generated an electrical response, characterizing them as a gas sensor.

### 2.4. Gas sensors

The sensory measurements were made through the study of current versus time curves ( $I$  vs  $t$ ). In the controlled gas measurement system, an inert nitrogen ( $\text{N}_2$ ) flow is initially applied to stabilize the sample and create a baseline.

After this initial stabilization, the  $\text{NH}_3$  flux is released by drag with the same  $\text{N}_2$ , now the ammonia flux acting on

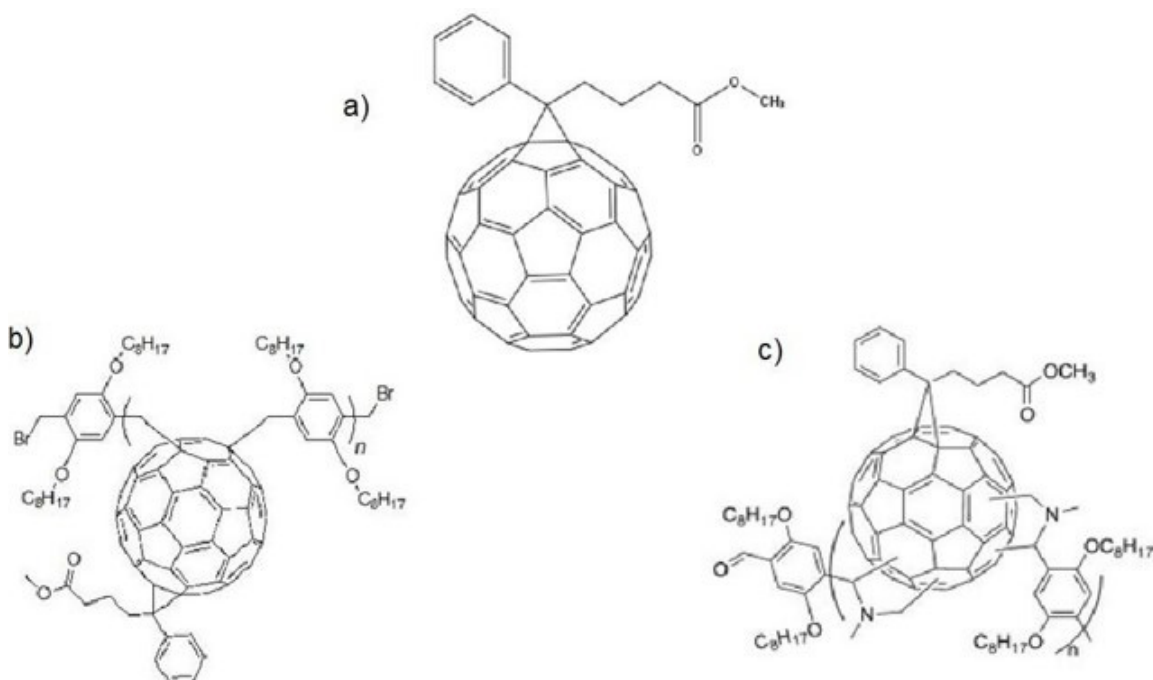


**Figure 1.** Chemical structure of a) PCBM; b) OPCBMMB; c) PPCBMB.

the sensor substrate, an interaction that generates a change in the electrical current registered in the device. This process between the flow of NH<sub>3</sub> vapor and pure N<sub>2</sub> (inert gas) is alternated so that a visible electrical interaction is observed. The process is alternated in cycles of 10 minutes at a constant flow of 60N.L/h. Figure 4 represents a schematic of the system used for the sensory measurements.

### 3. Results and Discussions

#### 3.1. Sensor responses

The experiment was carried out in cycles of 10 minutes, alternating between the baseline of N<sub>2</sub> and NH<sub>3</sub>. During the entire process, the samples were subjected to a constant

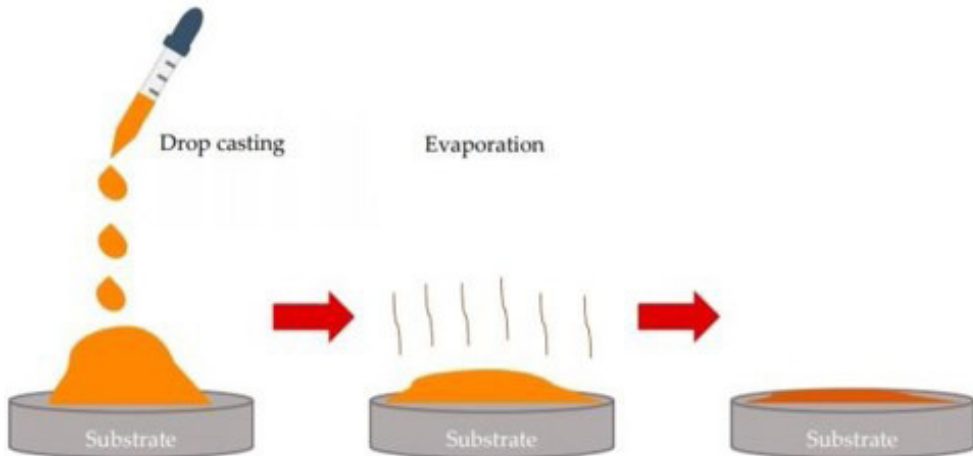


Figure 2. Scheme showing the Drop casting deposition process<sup>11</sup>.

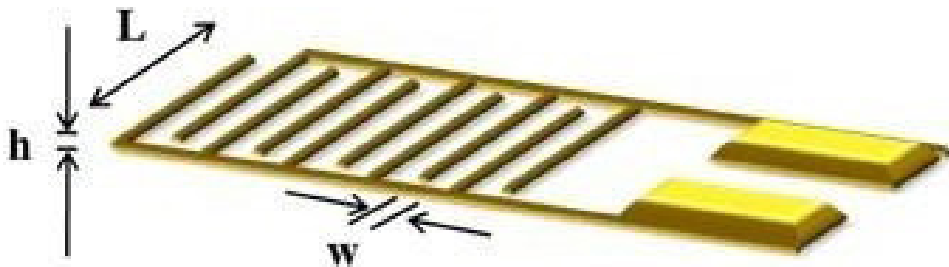


Figure 3. Representation of a golden interdigitate electrode with  $N = 10^{17}$ .

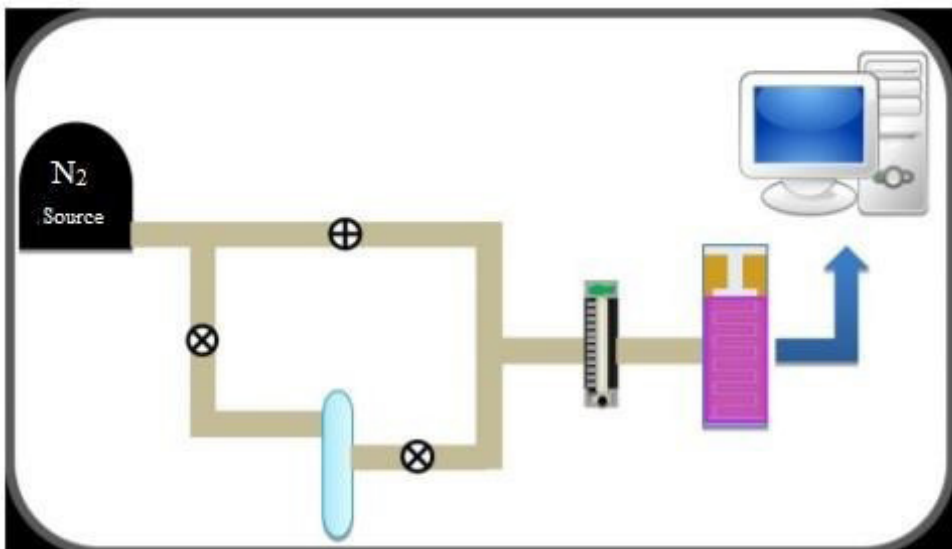
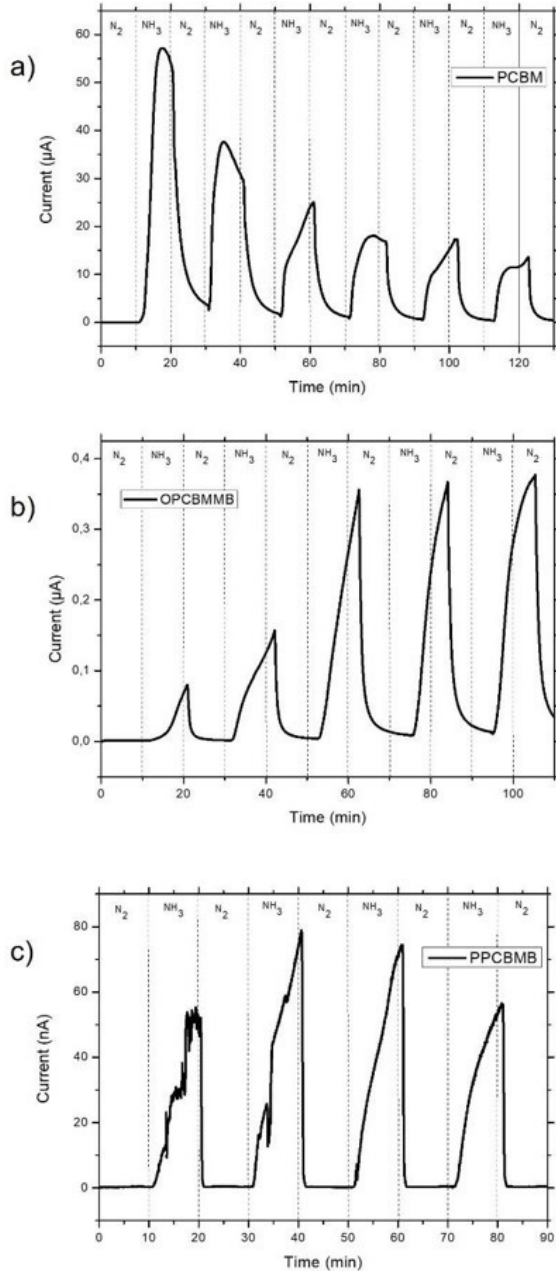


Figure 4. Representation of the sensory measurements system<sup>18</sup>.

voltage of 5 V. Figure 5 displays the results obtained for the three materials.

The graphs reveals that the three materials responded to the presence of  $\text{NH}_3$ , showing a large increase in the measured current. The highest response is observed on PCBM, which



**Figure 5.**  $I$  vs  $t$  curves for the sensor devices with Drop casting films of: a) PCBM; b) OPCBMMB; c) PPCBMB.

**Table 1.** Current peaks observed at each cycle for the studied materials.

| Current peaks | 1 <sup>st</sup> cycle | 2 <sup>nd</sup> cycle | 3 <sup>rd</sup> cycle | 4 <sup>th</sup> cycle |
|---------------|-----------------------|-----------------------|-----------------------|-----------------------|
| PCBM          | 57 $\mu\text{A}$      | 38 $\mu\text{A}$      | 25 $\mu\text{A}$      | 18 $\mu\text{A}$      |
| OPCBMMB       | 0.08 $\mu\text{A}$    | 0.16 $\mu\text{A}$    | 0.36 $\mu\text{A}$    | 0.37 $\mu\text{A}$    |
| PPCBMB        | 55 nA                 | 78 nA                 | 74 nA                 | 56 nA                 |

had a peak of 57  $\mu\text{A}$ , followed by OPCBMMB, with a peak of 0.37  $\mu\text{A}$ . PPCBMB showed the lowest peak, 78 nA.

As these materials have different size (PCBM, oligo-fullerene and poly-fullerene), it is possible to observe variations in the behavior of the structures of each material, and after being exposed to ammonia vapor, the PCBM films showed a fast response in contact with the analyte, decreasing electrical stimulation over time.

As for oligo and poly fullerenes, we observed a different response from PCBM. OPCBMMB showed an increase in electrical stimulus at each cycle, while PPCBMB showed an apparently continuous response without major changes during exposure cycles. This performance in gas response for the three materials can be explained by the fact that they PCBM in common in their structure and that they are n-type materials, which reacts favorably with  $\text{NH}_3$ , increasing the semiconductor nature of the material, revealing current peaks when exposed to gas<sup>19,20</sup>, we verified in the ammonia responses that the oligo and poly fullerenes have a more consistent response to each cycle, keeping the current at close values, according to Table 1. Interestingly, although the response is less marked in the first cycles, OPCBMMB showed a more consistent response at 60 and 80 minutes (3<sup>rd</sup> and 4<sup>th</sup> cycles).

Another important factor is the technique used in this work. The Drop casting technique has a low level of control in the materials organization, which results in a film with low homogeneity, as stated in previous works from Kanoun<sup>11</sup>, Pimentel<sup>12</sup> and Castro<sup>21</sup>. This can create void on the structure, capable of absorbing  $\text{NH}_3$  molecules by weak chemical interaction<sup>20</sup>. The materials then capture the gas charges, which then participate in the conduction process<sup>22,23</sup>. Observing the graphs, it is also possible to verify that, not only the materials responded to the  $\text{NH}_3$ , but also this response is reproducible. The materials showed the ability to repeat the gas response, indicating that sensor devices made from them can be reused<sup>24,25</sup>.

### 3.2. DC characterization

Figure 6 shows  $I$  vs  $V$  characteristic curves. The samples were subjected to a voltage ranging from -15 V to 15 V, with a 0.5 V step. The process was done before and after exposure to  $\text{NH}_3$ , in order to observe possible changes in the electrical behavior of the materials, and to check if the process is reversible.

The linear curves of current ( $I$ ) vs. voltage ( $V$ ), represented in Figure 6 show that the materials presented an ohmic behavior, due to contact with the Au/film/Au configuration<sup>26</sup>, especially in the lower voltage regions. Ohmic contacts, such as those observed, have the characteristic of not influencing the density of carriers in the studied material volume when an electrical voltage is applied<sup>26,27</sup>. This feature allows us to

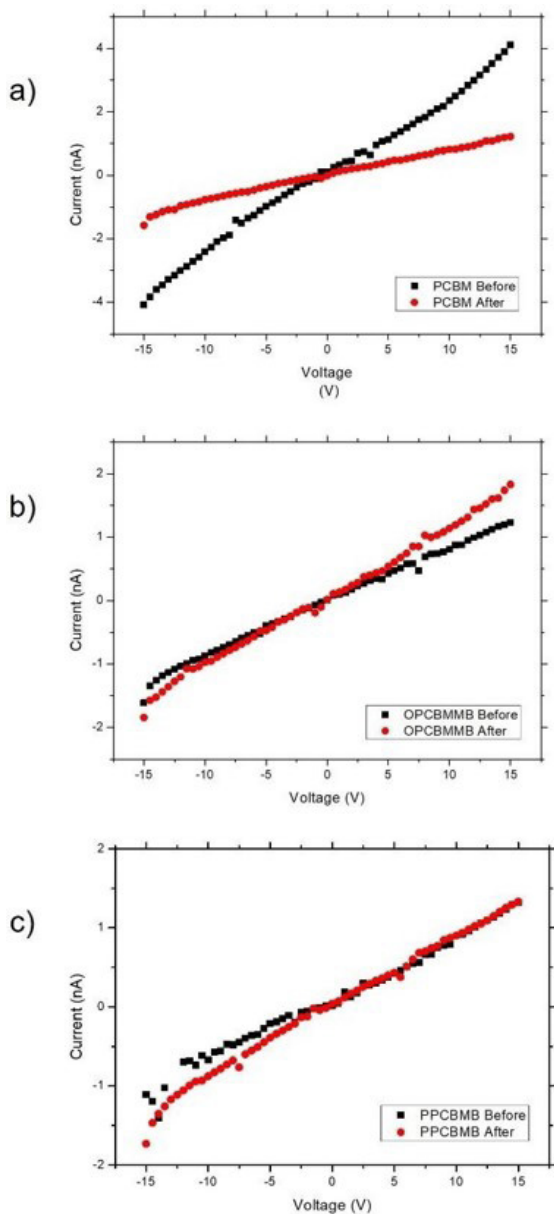


**Figure 6.**  $I$  vs  $V$  curves before and after exposure to  $\text{NH}_3$  for: a) PCBM; b) OPCBMMB; c) PPCBMB.

obtain information about these materials, such as electrical conductivity<sup>28</sup>.

This observed behavior can be described by the linear equation ( $y = ax + b$ ), with  $b = 0$ . From Ohm's Law, with Equations 1 and 2, it is possible to determine the resistance ( $R$ ) and the electrical conductivity ( $\sigma$ ), since the conductivity is the inverse of resistivity ( $\rho$ ), ( $\sigma = 1/\rho$ ).

$$V = R \cdot i \quad (1)$$

$$R = K \cdot \rho \quad (2)$$

In Equation 2,  $K$  is the cell constant, defined by the geometry of the used IDE. In this work, the IDE used has a cell constant with a value of  $5.1 \text{ m}^{-1}$ , as defined in

**Table 2.** Material conductivities before and after exposure to  $\text{NH}_3$ .

| Active Layer | Conductivity ( $\text{S m}^{-1}$ ) before exposure to $\text{NH}_3$ | Conductivity ( $\text{S m}^{-1}$ ) after exposure to $\text{NH}_3$ |
|--------------|---|--|
| PCBM         | $1.26 \times 10^{-9}$   | $4.20 \times 10^{-10}$   |
| OPCBMMB      | $4.38 \times 10^{-10}$  | $5.61 \times 10^{-10}$   |
| PPCBMB       | $4.96 \times 10^{-10}$  | $4.63 \times 10^{-10}$   |

previous works<sup>18</sup>, following the model of Olthuis et al.<sup>29</sup>. Table 2 disposes the conductivity values to the materials before and after exposure to  $\text{NH}_3$ .

Observing the graphs, it is possible to state that the three materials kept their ohmic behavior. However, although OPCBMMB and PPCBMB maintained similar conductivity values, PCBM showed a considerable reduction to its value. This might be due to the tendency of fullerenes to react permanently with amines, which would explain the behavior of PCBM<sup>30</sup>. The oligomer and polymer probably react less due to the steric blocking of permanent reactions by the comonomers in the polymer structures, thereby maintaining their structures and sensitivity to ammonia over time. These reactions may change with light and this will be part of a future study.

When analyzing the data in Table 2, we verified that before exposure to the gas, all materials have low conductivity, with PCBM presenting the highest conductivity value among them<sup>31,32</sup>, about 1 order of magnitude higher. When exposed to gas, we found that the structure of pure PCBM, when in contact with  $\text{NH}_3$  vapor, decreased its electrical conductivity by an order of magnitude, due to a possible nucleophilic reaction of  $\text{NH}_3$  with PCBM, reducing its ability to exchange electrical charges, which can be seen in Figure 5, observing the drop in current peak over time. The other materials did not undergo major changes, maintaining their similar conductivities before and after exposure to the gas. Both OPCBMMB and PPCBMB have ramifications that can block the permanent chemistry with the gas, which reduces interactions with ammonia, but allows a response reproducibility over time, a fact that can be compared to PCBM in Figure 5, where these materials showed consistent results throughout each cycle<sup>33,34</sup>.

## 4. Conclusions

Analyzing the results obtained from this work, we observe the behavior of PCBM, OPCBMMB and PPCBMB when immersed in an ammonia atmosphere, verifying the electrical response generated by the gas stimulus. It is noted that PCBM, despite having the highest peak among the materials studied, shows a drop in its electrical response at each cycle, due to a possible nucleophilic reaction between the gas and the material, which reduces its ability to exchange electrical charges. This phenomenon is not observed in OPCBMMB and PPCBMB, as they present ramification capable of blocking these permanent reactions with the gas, which reduces their interaction capacity, resulting in smaller, but more consistent response peaks.

By analyzing the conductivity curves ( $I$  vs  $V$ ) before and after the interaction with ammonia, it can be observed that the three materials studied preserved their ohmic behavior



after ammonia stimuli, with OPCBMMB and PPCBMB maintaining very close conductivity values, while PCBM showed a significant reduction in its electrical conductivity, about an order of magnitude, but also maintaining its ohmic behavior

The results obtained shows that these materials present favorable conditions for the production of NH<sub>3</sub> sensors, as they all react to the gas stimulus, and are capable of reproducing the response, without losing their electrical properties. In this context, we highlight OPCBMMB and PPCBMB, as they are able to reproduce the results with better consistency.

## 5. Acknowledgements

This study was financed in part by the Coordenação de Aperfeiçoamento de Pessoal de Nível Superior – Brasil (CAPES) – Finance Code 001.

## 6. References

- De Paoli MA, Menescal RK. Polímeros orgânicos condutores de corrente elétrica: uma revisão. *Quim Nova*. 1986;9(2):133-40.
- Kroto HW, Heath JR, O'Brien SC, Curl RF, Smalley RE. C<sub>60</sub>: buckminsterfullerene. *Nature*. 1985;318(6042):162-3. <http://dx.doi.org/10.1038/318162a0>.
- Venegas Romero JG. Síntese de fullerenos (C<sub>60</sub> e C<sub>70</sub>) e nanotubos de carbono de parede simples por pirólise em plasma de hélio, e sua caracterização por espectroscopia IV, UV-Vis, DRX, adsorção de gases, espectroscopia Raman, MEV e MET [tese]. Campinas: Universidade Estadual de Campinas; 2002.
- Hiorns RC, Cloutet E, Ibarboure E, Vignau L, Lemaitre N, Guillerez S, et al. Main-chain fullerene polymers for photovoltaic devices. *Macromolecules*. 2009;42(10):3549-58. <http://dx.doi.org/10.1021/ma900279a>.
- Ramanitra HH, Santos Silva H, Bregadiolli BA, Khoukh A, Combe CMS, Dowland SA, et al. Synthesis of main-chain poly(fullerene)s from a sterically controlled azomethine ylide cycloaddition polymerization. *Macromolecules*. 2016;49(5):1681-91. <http://dx.doi.org/10.1021/acs.macromol.5b02793>.
- Šutka A, Kodu M, Pärna R, Saar R, Juhneviča I, Jaanisoo R, et al. Orthorhombic CaFe<sub>2</sub>O<sub>4</sub>: a promising p-type gas sensor. *Sens Actuators B Chem*. 2016;224:260-5. <http://dx.doi.org/10.1016/j.snb.2015.10.041>.
- Bundgaard E, Krebs FC. Low band gap polymers for organic photovoltaics. *Sol Energy Mater Sol Cells*. 2007;91(11):954-85. <http://dx.doi.org/10.1016/j.solmat.2007.01.015>.
- Li Z, Ho Chiu K, Shahid Ashraf R, Fearn S, Dattani R, Cheng Wong H, et al. Toward improved lifetimes of organic solar cells under thermal stress: substrate-dependent morphological stability of PCDTBT:PCBM Films and Devices. *Sci Rep*. 2015;5(1):15149. <http://dx.doi.org/10.1038/srep15149>.
- Krupa SV. Effects of atmospheric ammonia (NH<sub>3</sub>) on terrestrial vegetation: A review. *Environ Pollut*. 2003;124(2):179-221. [http://dx.doi.org/10.1016/S0269-7491\(02\)00434-7](http://dx.doi.org/10.1016/S0269-7491(02)00434-7).
- Sutton MA, Dragosits U, Tang YS, Fowler D. Ammonia emissions from non-agricultural sources in the UK. *Atmos Environ*. 2000;34(6):855-69. [http://dx.doi.org/10.1016/S1352-2310\(99\)00362-3](http://dx.doi.org/10.1016/S1352-2310(99)00362-3).
- Kanoun O, Müller C, Benchirouf A, Sanli A, Dinh T, Al-Hamry A, et al. Flexible carbon nanotube films for high performance strain sensors. *Sensors*. 2014;14(6):10042-71. <http://dx.doi.org/10.3390/s140610042>.
- Pimentel LC. Filmes finos multicamadas de polímeros condutores, nanotubos de carbono e fullerenos modificados para aplicação na conversão de energia solar [tese]. Campinas: Universidade Estadual de Campinas; 2012.
- Falke S, Eravuchira P, Materny A, Lienau C. Raman spectroscopic identification of fullerene inclusions in polymer/fullerene blends. *J Raman Spectrosc*. 2011;42(10):1897-900. <http://dx.doi.org/10.1002/jrs.2966>.
- Kumar AKS, Zhang Y, Li D, Compton RG. A mini-review: how reliable is the drop casting technique? *Electrochem Commun*. 2020;12:106867. <http://dx.doi.org/10.1016/j.elecom.2020.106867>.
- Ramanitra HH, Dowland SA, Bregadiolli BA, Salvador M, Santos Silva H, Bégue D, et al. Increased thermal stabilization of polymer photovoltaic cells with oligomeric PCBM. *J Mater Chem C Mater Opt Electron Devices*. 2016;4(34):8121-9. <http://dx.doi.org/10.1039/C6TC03290G>.
- Stephen M, Ramanitra HH, Santos Silva H, Dowland S, Bégue D, Genevičius K, et al. Sterically controlled azomethine ylide cycloaddition polymerization of phenyl-C<sub>61</sub>-butyric acid methyl ester. *Chem Commun*. 2016;52(36):6107-10. <http://dx.doi.org/10.1039/C6CC01380E>.
- Bittencourt JC, Santana Gois BH, Rodrigues de Oliveira VJ, Silva Agostini DL, Almeida Olivati C. Gas sensor for ammonia detection based on poly(vinyl alcohol) and polyaniline electrospun. *J Appl Polym Sci*. 2019;136(13):47288. <http://dx.doi.org/10.1002/app.47288>.
- Silva EA. Efeito da adição de moléculas anfífilicas na formação de filmes Langmuir e Langmuir-Blodgett de derivados alquilados do politiofeno: aplicação em sensores [dissertação]. Presidente Pudente: Universidade Estadual Paulista; 2014.
- Chuang MY, Chen JN, Zan HW, Lu CJ, Meng HF. Modulated gas sensor based on vertical organic diode with blended channel for ppb-regime detection. *Sens Actuators B Chem*. 2016;230:223-30. <http://dx.doi.org/10.1016/j.snb.2016.02.030>.
- Chen Y, Xie G, Xie T, Liu Y, Du H, Su Y, et al. Thin film transistors based on poly(3-hexylthiophene)/[6,6]-phenyl C<sub>61</sub> butyric acid methyl ester hetero-junction for ammonia detection. *Chem Phys Lett*. 2015;638:87-93. <http://dx.doi.org/10.1016/j.cplett.2015.07.026>.
- Castro SVF. Sensor voltamétrico para detecção de trinitrotolueno baseado em nanocompósito de óxido de grafeno reduzido e nanotubos de carbono [dissertação]. Uberlândia: Universidade Federal de Uberlândia; 2018.
- Kumar C, Rawat G, Kumar H, Kumar Y, Kumar A, Prakash R, et al. Electrical and ammonia gas sensing properties of PQT-12/CdSe quantum dots composite-based organic thin film transistors. *IEEE Sens J*. 2018;18(15):6085-91. <http://dx.doi.org/10.1109/JSEN.2018.2845873>.
- Kumar C, Rawat G, Kumar H, Kumar Y, Prakash R, Jit S. Electrical and ammonia gas sensing properties of poly(3, 3'-dialkylquaterthiophene)-based organic thin film transistors fabricated by floating-film transfer method. *Org Electron*. 2017;48:53-60. <http://dx.doi.org/10.1016/j.orgel.2017.05.040>.
- Park MS, Meresa AA, Kwon C, Kim FS. Selective wet-etching of polymer/fullerene blend films for surface- and nanoscale morphology-controlled organic transistors and sensitivity-enhanced gas sensors. *Polymers*. 2019;11(10):1682. <http://dx.doi.org/10.3390/polym11101682>.
- Cheng H, Lin W, Wu F, Cheng H, Lin W, Wu F. Effects of solvents and vacancies on the electrical hysteresis characteristics in regioregular poly(3-hexylthiophene) organic thin-film transistors. *Appl Phys Lett*. 2009;94(22):223302. <http://dx.doi.org/10.1063/1.3148332>.
- Sze SM, Kwok KN. *Physics of semiconductor devices*. Hoboken: Wiley; 2005.
- Tomozawa H, Braun D, Phillips SD, Worland R, Heeger AJ, Kroemer H. Metal-polymer schottky barriers on processible polymers. *Synth Met*. 1989;28(1-2):687. [http://dx.doi.org/10.1016/0379-6779\(89\)90591-2](http://dx.doi.org/10.1016/0379-6779(89)90591-2).
- Audenaert M, Gusman G, Deltour R. Electrical conductivity in doped polyacetylene. *Phys Rev B Condens Matter*. 1981;24(12):7380-2. <http://dx.doi.org/10.1103/PhysRevB.24.7380>.

29. Olthuis W, Sprenkels AJ, Bomer JG, Bergveld P. Planar interdigitated electrolyte-conductivity sensors on an insulating substrate covered with Ta<sub>2</sub>O<sub>5</sub>. *Sens Actuators B Chem.* 1997;43(1-3):211-6. [http://dx.doi.org/10.1016/S0925-4005\(97\)00157-3](http://dx.doi.org/10.1016/S0925-4005(97)00157-3).
30. Miller GP. Reactions between aliphatic amines and [60] fullerene: a review. *C R Chim.* 2006;9(7-8):952-9. <http://dx.doi.org/10.1016/j.crci.2005.11.020>.
31. Roncaselli LKM. Estudo e caracterização de filmes nanoestruturados de derivados de poli-fulerenos [tese]. Presidente Prudente: Universidade Estadual Paulista; 2021.
32. Roncaselli LKM, Silva EA, Ramanitra HH, Stephen M, Simões AVS, Bégué D, et al. Study of the effect of solvent on the conductivity of langmuir-schaefer films of poly(fullerene)s. *Mater Res.* 2021;24(Suppl. 1):e20210028. <http://dx.doi.org/10.1590/1980-5373-mr-2021-0028>.
33. Lv A, Pan Y, Chi L. Gas sensors based on polymer field-effect transistors. *Sensors.* 2017;17(12):213. <http://dx.doi.org/10.3390/s17010213>.
34. Yang Y, Sun L, Ou J, He Y, Lin X, Yuan Z, et al. Plasmonic effects and the morphology changes on the active material P3HT:PCBM used in polymer solar cells using Raman spectroscopy. *J Raman Spectrosc.* 2016;47(8):888-94. <http://dx.doi.org/10.1002/jrs.4917>.